J. Appl. Glycosci., **67**, 73–78 (2020)
doi: 10.5458/jag.jag.JAG-2020_0002
©2020 The Japanese Society of Applied Glycoscience

Regular Paper

Single Amino Acid Mutation of Pyranose 2-Oxidase Results in Increased Specificity for Diabetes Biomarker 1,5-Anhydro-D-Glucitol

(Received February 19, 2020; Accepted April 14, 2020)
(J-STAGE Advance Published Date: May 23, 2020)

Takahiro Fujii,[1,2] Kiyohiko Igarashi,[2,3,†] and Masahiro Samejima[2,4]

[1]*Ikeda Food Research Co., Ltd.*
(*95–7 Minoshima, Fukuyama Hiroshima 721–0956, Japan*)
[2]*Department of Biomaterial Sciences, Graduate School of Agricultural and Life Sciences, The University of Tokyo*
(*1–1–1 Yayoi, Bunkyo-ku, Tokyo 113–8657, Japan*)
[3]*VTT Technical Research Centre of Finland*
(*P.O.Box 1000, Tietotie 2, Espoo FI-02044, Finland*)
[4]*Faculty of Engineering, Shinshu University*
(*4–17–1 Wakasato, Nagano City, Nagano 380–8553, Japan*)

Abstract: Pyranose 2-oxidases catalyze the oxidation of various pyranose sugars at the C2 position. However, their potential application for detecting sugars other than glucose in blood is hindered by relatively high activity towards glucose. In this study, in order to find a mutant enzyme with enhanced specificity for 1,5-anhydro-D-glucitol (1,5-AG), which is a biomarker for diabetes mellitus, we conducted site-directed mutagenesis of pyranose 2-oxidase from the basidiomycete *Phanerochaete chrysosporium* (*Pc*POX). Considering the three-dimensional structure of the substrate-binding site of *Pc*POX and the structural difference between glucose and 1,5-AG, we selected alanine 551 of *Pc*POX as a target residue for mutation. Kinetic studies of the 19 mutants of *Pc*POX expressed as recombinant proteins in *E. coli* revealed that the ratio of k_{cat}/K_m for 1,5-AG to k_{cat}/K_m for glucose was three times higher for the A551L mutant than for wild-type *Pc*POX. Although the A551L mutant has lower specific activity towards each substrate than the wild-type enzyme, its increased specificity for 1,5-AG makes it a promising lead for the development of POX-based 1,5-AG detection systems.

Key words: 1,5-anhydro-D-glucitol, pyranose 2-oxidase, *Phanerochaete chrysosporium*, diabetes

INTRODUCTION

Diabetes is a metabolic disease characterized by hyperglycemia, which can lead to eye damage, kidney disease and increased susceptibility to infections, and it is predicted to be the 7th leading cause of death in the world by 2030. Control of blood glucose level is critical for diabetes treatment, and considerable efforts have been made to identify biomarkers that reflect blood glucose levels.[1)2)3)4)] Among them, hemoglobin A1c and glycated albumin reflect average blood glucose levels during the previous few months and the previous 2 weeks, respectively. However, these time scales are too slow to assess treatment effects. On the other hand, 1,5-anhydro-D-glucitol (1,5-AG) responds more rapidly, reflecting average blood glucose level over the previous few days.[5)]

1,5-AG, the 1-deoxy derivative of glucopyranose, is one of the principal polyols in human blood, and 99.9 % of it is reabsorbed by the kidney.[6)] In diabetic hyperglycemia, the renal absorption of 1,5-AG is competitively inhibited by glucose, and so the 1,5-AG concentration in blood is decreased. The concentration of 1,5-AG in human blood can be determined by biochemical methods, e.g., by using an oxidase to generate hydrogen peroxide from 1,5-AG, coupled to horseradish peroxidase to provide a measurable absorbance change, but few oxidases exhibit sufficient activity or selectivity for 1,5-AG, because this compound lacks reducing-end.[7)]

However, pyranose 2-oxidases (POXs, EC 1.1.3.10) show high reactivity towards 1,5-AG and are candidates for monitoring hyperglycemia.[8)9)] POXs oxidize substrates at the C2 position, producing 2-ketoaldose and hydrogen peroxide from molecular oxygen as shown in Fig. 1.[10)11)] However, they recognize not only 1,5-AG, but also glucose, so enzymatic depletion of glucose is used in a commercial bioassay (*c.f.* GlycoMark Assay) to increase performance, though this makes the assay more complex.[6)] Therefore, there is a need to create or discover new POXs with higher specificity for 1,5-AG.

Here, we focused on POX from the basidiomycete *Phanerochaete chrysosporium* (*Pc*POX), as its structure has already been reported, the protein can be expressed in *Escherichia coli*,[12)13)] and this enzyme has thermal stability

[†]Corresponding author (Tel. +81–3–5841–5258, Fax. +81–3–5841–5257, E-mail: aquarius@mail.ecc.u-tokyo.ac.jp, ORCID ID: 0000-0001-5152-7177).
Abbreviations: 1,5-AG, 1,5-anhydro-D-glucitol; POX, pyranose oxidase; Pc, Phanerochaete chrysosporium; WT, wild-type.
This is an open-access paper distributed under the terms of the Creative Commons Attribution Non-Commercial (by-nc) License (CC-BY-NC4.0: https://creativecommons.org/licenses/by-nc/4.0/).

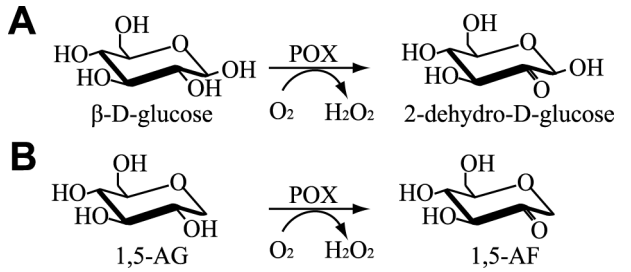

Fig. 1. Structures of β-D-glucose (A) and 1,5-AG (B), and proposed C-2 oxidation mechanism by *Pc*POX.
*Pc*POX catalyzes the oxidation of 1,5-AG at C2, producing hydrogen peroxide and 2-ketoaldose, 1,5-anhydrofructose (1,5-AF).

enough for clinical application. *Pc*POX is a tetrameric flavoprotein that contains a binding site for flavin adenine dinucleotide (FAD), and shows activity towards various kinds of aldose, using molecular oxygen or various quinones as electron acceptors.[12)14)15)] Based on a consideration of the three-dimensional structure of the substrate-binding site of *Pc*POX and the structural difference between glucose and 1,5-AG, we selected alanine 551 of *Pc*POX as a target residue for mutation with the aim of improving the 1,5-AG/glucose activity ratio, since this residue is likely to be important for recognition of the C1 hydroxyl group of glucose. We used site-directed mutation to replace this residue with 19 other amino acids. The obtained *Pc*POX mutants were simply purified by use of a Histidine-tag, and their substrate specificity and kinetic values were determined.

MATERIALS AND METHODS

Cloning of cDNA encoding pyranose 2-oxidase. *P. chrysosporium* strain K-3[16)] was grown on the Kremer and Wood medium[17)] containing 2 % cellulose (CF11, Whatman Laboratory Products, Fairfield, USA) as a sole carbon source, based on a previous report.[18)] After 3 days of cultivation, mycelia were separated from the culture filtrate on a glass filter membrane (ADVANTEC GA-100, Toyo-Roshi Kaisha Ltd., Tokyo, Japan) and frozen with liquid nitrogen. Total RNA was extracted from the mycelial powder using ISOGEN (Nippon Gene Co., Ltd., Tokyo, Japan), and first-strand cDNA was synthesized as described previously. Oligonucleotide primers used for amplification of *pcpox* gene, F1: TTTCATATGTTTCTTGACACCACACCA and R1: TTTAAGCTTTTAATGATGATGATGATGATGATGGCCGCGGTGACGACCAAA, were designed based on the *P. chrysosporium* genome information (GenBank accession no. AY522922.[10)13)] The amplified *pcpox* gene was ligated to pCR™2.1-TOPO® vector (Zero Blunt TOPO PCR Cloning Kit for Sequencing, Invitrogen, Tokyo, Japan), and the resulting plasmid was used for JM109 heat-shock transformation according to the manufacturer's instructions. The nucleotide sequences of the inserted genes were analyzed as described previously.[19)]

Production and purification of* Pc*POX. For the preparation of the expression vector plasmid, *pcpox* gene was amplified by PCR using a set of primers, F2: AAGGAGATATACATATGTTTCTTGACACCACACCATTC and R2: GTGCGGCCGCAAGCTTTTAATGATGATGATGATGATGGCCGCGGTGACGACCAAACTTCG, to introduce 15 bases (underlined) that correspond to the multicloning site sequence of pET-27b(+) vector. The obtained fragment was ligated into pET-27b(+) digested with NdeI and HindIII by using an In-Fusion® HD Cloning Kit (Takara Bio, Otsu, Japan). The construct was used for BL21(DE3) heat-shock transformation, and the cells were cultured in 200 μL of LB for 60 min at 37 ºC after the heat shock. The recovered cells were transplanted on LB Agar plates containing 50 μg/mL kanamycin. Selected transformants were picked up after 16 h and used for sequence analysis.

For protein expression, the selected colony was inoculated into 5 mL liquid LB medium containing 0.02 mM riboflavin, and induced for 24 h at 16 ºC with 0.1 mM IPTG. Cells were harvested by centrifugation at 8,000 × G, 4 ºC for 3 min, and the pellet was disrupted with Bugbuster (Merck Millipore, Tokyo, Japan). The lysate, making up the total cell fraction, was centrifuged (16,000 × G, 20 min, 4 ºC) to isolate the soluble fraction. The cleared lysate supernatant was applied to a His-spin column (GE Healthcare, Tokyo, Japan) pre-equilibrated with binding buffer composed of 50 mM sodium phosphate buffer (pH 8.0) containing 0.5 M NaCl, incubated on ice for 60 min, and centrifuged at 300 × G, 4 ºC for 30 seconds. The column was washed with wash buffer, 50 mM sodium phosphate buffer (pH 8.0), containing 0.5 M NaCl and 20 mM imidazole. The target protein was eluted with elution buffer, 50 mM sodium phosphate buffer pH 8.0, 0.5 M NaCl, 0.5 M imidazole. Eluate fractions were subjected to activity assay.

Preparation of* Pc*POX mutants. The QuikChange method[20)] was used for site-directed mutagenesis, with plasmid extracted from the selected transformant as a template and degenerate primers, F3: GACACCCGGCCTCNNNCTGCACCTCGCGGGCAC and R3: GTGCCCGCGAGGTGCAGNNNGAGGCCGGGTGTC, where N means any nucleotide. Transformation of *E. coli*, selection of transformants, protein expression and purification were carried out in the same way as described for wild-type *Pc*POX. The methods described under "Production and purification of *Pc*POX" were also used for the purification of A551N and A551L mutants.

Activity assay. Enzyme activities towards 10 mM 1,5-AG, glucose, maltose, xylose and galactose in 50 mM sodium phosphate buffer pH 7.0 were determined by means of dichlorophenolindophenol (DCIP) assay, using an absorption coefficient of 16.3 $mM^{-1}cm^{-1}$ at 600 nm.[21)] To obtain kinetic parameters, enzyme activities were determined by measuring the amount of H_2O_2 produced during substrate oxidation, using an absorption coefficient of 5.3 $mM^{-1}cm^{-1}$ at 505 nm. The reaction mixture contained 50 mM sodium phosphate buffer pH 7.0, 0.5 mM 4-aminoantipyrine, 0.5 mM phenol, 5 U/mL horseradish peroxidase, and glucose or 1,5-AG. Values of k_{cat}/K_m were calculated according to the Michaelis-Menten equation, using DeltaGraph (Ver. 7.0, RockWare).

RESULTS AND DISCUSSION

Because of their broad substrate specificity,[8)9)] POXs

have been considered for the detection of various sugars or glucose-related compounds. However, for quantitative detection of 1,5-AG in blood, the high activity of POXs towards glucose is a critical problem. According to the crystal structure of *Pc*POX-glucose complex (PDB ID: 4MIH),[12] the C1 hydroxyl group of glucose is hydrogen-bonded to the main-chain carbonyl group of Ala551 in addition to the side-chain of catalytic histidine (His553), and no direct interaction can be found with other amino acid residues (Fig. 2A). Although Ala551 is located close to the catalytic residue His553 and is highly conserved among known fungal POXs, it is substituted with valine or other amino acids in some other enzymes (Fig. 2B), suggesting that mutation of Ala551 would not necessarily eliminate POX activity. Therefore, we generated 19 *Pc*POX mutants with mutation of Ala551 and compared their activities towards 1,5-AG and glucose.

Fortunately, all the *Pc*POXs including WT were successfully produced as active recombinant proteins in *E. coli* (Fig. 3A), and were easily purified on a His-tag column, while the specific activities of these enzymes were generally low comparing to WT as shown in Fig. 3B with log scale y-axis. Since WT has an alanine, one of smallest amino acids, at the position, the specific activity towards glucose, 1,5-AG, maltose, xylose and galactose is retained when A551 is mutated to amino acids with smaller side chain such as proline (P), serine (S), cysteine (C), and threonine (T). Arginine (R) mutation also retains activity, possibly because of its flexibility in conformation of the side chain. On the other hand, other mutations showed significant loss of specific activity towards glucose (approximately 1/50). For instances, when A551 was mutated to negatively charged amino acids glutamic acid (E) and aspartic acid (D), amphipathic amino acid methionine (M), and bulky hydrophobic amino acids, such as phenylalanine (F), tyrosine (Y), and tryptophan (W), the specific activities were decreased significantly. In addition, we evaluated kinetic assays of A551L mutant and A551N mutant for determining their enzymatic parameters, and found out that their k_{cat}/K_m decreased significantly (Table 1). This experimental outcome indicates a lowering of mutants enzymatic activity, which coincides with the result of Fig. 3B. The A551 is located around the catalytic histidine (His553). *Pc*POX structure may be distorted by the interaction between negatively charged amino acid introduced by A551 mutation and positively charged amino acid His553 or bulky hydrophobic amino acid insertion.

Then, we calculated relative activity to confirm substrate specificity towards 1,5-AG of WT and mutant *Pc*POXs. Relative activity is the ratio between the specific activity towards 1,5-AG and glucose, specific activity towards glucose of each specimen is taken as 100. Relative activity towards xylose, maltose, and galactose were also expressed, as was the case in 1,5-AG. As results of specific activity assay and calculation of relative activity, notably, the A551V, A551N, and A551L mutants showed higher relative activity towards 1,5-AG; in particular, A551N and A551L showed 1.5 and 3.6 times higher relative activity towards 1,5-AG, respectively, as shown in Fig. 3C. These

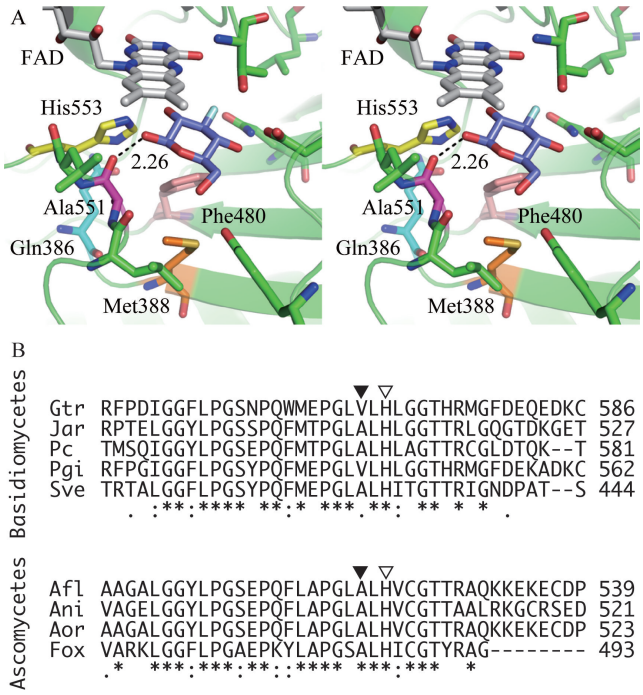

Fig. 2. Crystal structure of *Pc*POX active site (A), and sequence alignment of POXs from filamentous fungi (B).

(A) Structures of *Pc*POX and the bound substrate analog, 3-deoxy-3-fluoro-β-D-glucopyranose (G3F), were drawn from PDBID: 4MIH by PyMOL Molecular Graphics System, Version 0.99 Schrödinger, LLC.[8] The cofactor FAD, ligand G3F, catalytic residue His553, and amino acid residues around G3F are shown by stick representations with carbon atoms colored in gray, purple, yellow and green respectively. The amino acid residues Gln386, Met388, and Phe480 are shown by stick representations with carbon atoms colored in cyan, orange, and salmon, which are found around the methyl side chain of Ala551. The residue mutated in present study, Ala551, is also shown as a stick model with magenta carbon atoms. Non-carbon atoms are colored depending on the atom type. (B) POXs from basidiomycetes and ascomycetes were aligned using MAFFT.[28][29] The position of Ala551 in *Pc*POX is indicated by the black arrowhead. The white arrowhead indicates the position of the conserved catalytic histidine residue (His553 in *Pc*POX). The amino acid sequences of POXs in the alignments are those from *Gloeophyllum trabeum* (Gtr, ACM47528), *Jaapia argillacea* (Jar, KDQ54529), *Phanerochaete chrysosporium* (Pc, BAC20641), *Phanerochaete gigantea* (Pgi, Q6UG02), *Serendipita vermifera* (Sve, KIM30732), *Aspergillus flavus* (Afl, XP_002380126), *Aspergillus nidulans* (Ani, A4Q5B2E9), *Aspergillus oryzae* (Aor, XP_001818709) and *Fusarium oxysporum* (Fox, ENH71592).

mutants also showed higher relative activity towards xylose for A551N and towards xylose, maltose, and galactose for A551L, compared to glucose, but their relative activity was highest towards 1,5-AG among the substrates examined. Interesting feature is the asparagine (N) *vs*. aspartate (D), and glutamine (Q) *vs.* glutamate (E), which should have similar size of side chain, but different charges. Amino acids with charge-neutral, polar side chain (N or Q) have higher relative activity towards 1,5-AG than corresponding acidic amino acids (D or E). Both A551N and A551L showed higher K_m values for 1,5-AG, compared to WT (Fig. 4 and Table 1). However, if we compare the ratio of K_m for 1,5-AG to that for glucose, it is clear that these mutants are less active towards glucose and more specific for 1,5-AG, relative to WT. Moreover, the ratio of k_{cat}/K_m

Table 1. Kinetic parameters for glucose and 1,5-AG.

	Glucose			1,5-AG			K_m	k_{cat}/K_m
	K_m (mM)	k_{cat} (s^{-1})	k_{cat}/K_m ($s^{-1}mM^{-1}$)	K_m (mM)	k_{cat} (s^{-1})	k_{cat}/K_m ($s^{-1}mM^{-1}$)	1,5-AG / Glc	1,5-AG / Glc
WT	0.978±0.156	115±2	120	18.9±4.4	82.5±10.3	4.4	19	0.037
A551N	12.1±0.3	0.496±0.021	0.041	65.7±4.5	0.253±0.006	0.0038	5.4	0.094
A551L	3.44±1.15	0.00659±0.00129	0.0019	26.9±3.5	0.00696±0.00027	0.00026	7.8	0.135

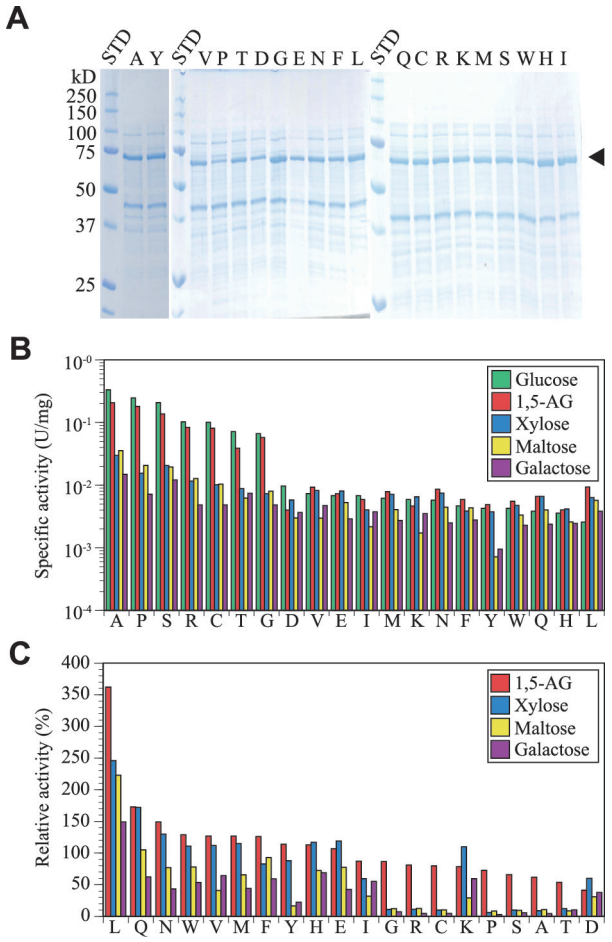

Fig. 3. Expression and activity comparison of WT (Ala551) and mutant *Pc*POXs (A551X).

(A) SDS-PAGE gel electrophoresis of crude *Pc*POXs. STD, Standard molecular weight marker proteins. The upper alphabets are single letter abbreviations for amino acids and they indicate WT (A) or 19 *Pc*POX mutants with mutation of Ala551. The black arrowhead points to *Pc*POXs band. (B) Specific activities for substrates (glucose, green; 1,5-AG, red; xylose, blue; maltose, yellow; galactose, purple). The y-axis is logarithmic scale. (C) Relative activities for 1,5-AG, xylose, maltose, and galactose. These expressed the ratio of specific activity for 1,5-AG, xylose, maltose, and galactose, as compared specific activity for glucose of each specimen, which is taken as 100.

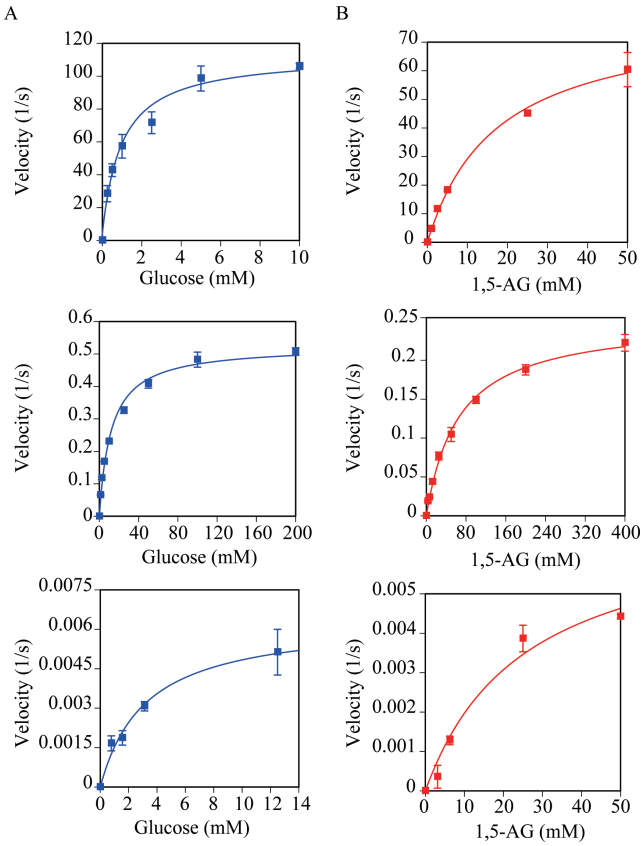

Fig. 4. Substrate dependence of oxidation rate by WT and mutant *Pc*POXs.

Oxidation rates of glucose (blue) and 1,5-AG (red) estimated by measuring hydrogen peroxide formation are shown in the left and right sections, respectively (WT, upper; A551N, middle; A551L, lower).

value for 1,5-AG to that for glucose was approximately 2.5 and 3.6 times higher for A551N and A551L, respectively, compared to WT. As stated previously, A551L mutant also showed 3.6 times higher relative activity towards 1,5-AG compared to glucose as shown in Fig. 3C, the value of relative activity was almost the same as the ratio of k_{cat}/K_m value for 1,5-AG to that for glucose as shown in Table 1. These results suggest that the experimental results obtained from Table 1 and Fig. 3C do not contradict each other and the mutations effectively decreased the affinity for glucose relative to that for 1,5-AG. When homology models of A551N and A551L were compared with the template *Pc*POX crystal structure (Fig. 5), these mutations appeared to exclude a water molecule interacting with the main-chain amide group of Ala551 and thus affect ligand binding. When we calculated the distance between the catalytic residue His553 and both ligands based on the WT crystal structure, we found that the distances between His553 and C1 or C2 of glucose and between His553 and C2 and C3 of 1,5-AG were about 3Å. Thus, we concluded that *Pc*POX might oxidize the C1 and C2 positions of glucose and the C2 and C3 positions of 1,5-AG. On the other hand, C2 of both ligands in the A551N mutant was located near His553, whereas C1 of glucose and C2 of 1,5-AG in the A551L mutant were located near His553. The results may

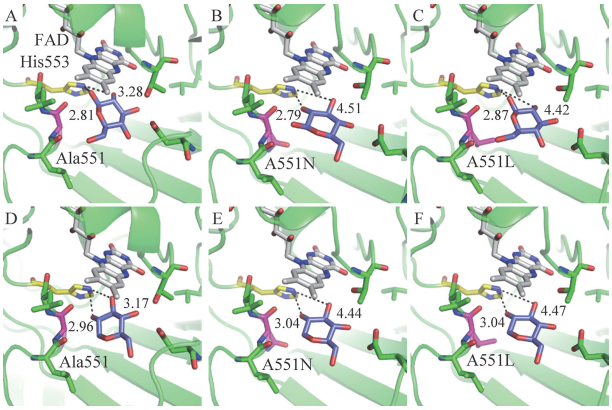

Fig. 5. The active site structures of WT (A, D: 4MIH.pdb) and mutant *Pc*POXs (B, C, E, F: homology models).

The images show molecular models of docked β-D-glucose (A-C) or 1,5-AG (D-F). The cofactor FAD, ligand β-D-glucose or 1,5-AG, catalytic residue His553, and amino acid residues around the ligand are shown by stick representations with carbon atoms colored in gray, purple, yellow and green, respectively. These images were created using AutoDock Vina[30] and PyMOL.

indicate that the A551N mutant oxidizes the C2 position of glucose and 1,5-AG, while the A551L mutant oxidizes the C1 position of glucose and the C2 position of 1,5-AG.

In conclusion, we selected the A551 residue of *Pc*POX as a target and created a series of mutants. Among them, the A551N and A551L mutants were less active towards glucose and more specific for 1,5-AG, relative to WT. Although their catalytic efficiency was decreased significantly and may be too low for clinical application,[22] we believe that they should be useful as leads for further optimization to obtain more active and 1,5-AG-specific enzymes by means of random mutagenesis[23][24][25] and high-throughput screening,[26][27] paving the way for clinical application.

CONFLICTS OF INTEREST

The authors declare no conflicts of interest.

ACKNOWLEDGMENTS

We are grateful to Drs. Akira Fukuda and Takuya Ishida of the University of Tokyo for their contribution in cloning cDNA encoding POX from *P. chrysosporium*, and Dr. Hironori Omura and Mr. Michinari Honda of Ikeda Food Research Co., Ltd. for useful discussions. This research was supported by a Grant-in-Aid for Innovative Areas from the Japanese Ministry of Education, Culture, Sports, and Technology (MEXT) (No. 18H05494), and an Impulsing Paradigm Change through Disruptive Technologies (ImPACT) grant from the Japan Science and Technology Agency (JST). K.I. thanks the Finnish Funding Agency for Innovation (TEKES) for the support of the Finland Distinguished Professor (FiDiPro) Program "Advanced approaches for enzymatic biomass utilization and modification (BioAD)".

REFERENCES

1) C. Diabetes, G. Complications Trial Research, D.M. Nathan, S. Genuth, J. Lachin, P. Cleary, O. Crofford, M. Davis, L. Rand, and C. Siebert: The effect of intensive treatment of diabetes on the development and progression of long-term complications in insulin-dependent diabetes mellitus. *N. Engl. J. Med.,* **329**, 977–986 (1993).

2) Y. Tahara and K. Shima: Kinetics of HbA1c, glycated albumin, and fructosamine and analysis of their weight functions against preceding plasma glucose level. *Diabetes Care,* **18**, 440–447 (1995).

3) M. Koga and S. Kasayama: Clinical impact of glycated albumin as another glycemic control marker. *Endocr. J.,* **57**, 751–762 (2010).

4) T. Suwa, A. Ohta, T. Matsui, R. Koganei, H. Kato, T. Kawata, Y. Sada, S. Ishii, A. Kondo, K. Murakami, T. Katabami, and Y. Tanaka: Relationship between clinical markers of glycemia and glucose excursion evaluated by continuous glucose monitoring (CGM). *Endocr. J.,* **57**, 135–140 (2010).

5) A. Sato: Indicators of glycemic control --hemoglobin A1c (HbA1c), glycated albumin (GA), and 1,5-anhydroglucitol (1,5-AG). *Rinsho Byori,* **62**, 45–52 (2014).

6) J.B. McGill, T.G. Cole, W. Nowatzke, S. Houghton, E.B. Ammirati, T. Gautille, and M.J. Sarno: Circulating 1,5-anhydroglucitol levels in adult patients with diabetes reflect longitudinal changes of glycemia: a U.S. trial of the GlycoMark assay. *Diabetes Care,* **27**, 1859–1865 (2004).

7) J.B. Buse, J.L. Freeman, S.V. Edelman, L. Jovanovic, and J.B. McGill: Serum 1,5-anhydroglucitol (GlycoMark): a short-term glycemic marker. *Diabetes Technol. Ther.,* **5**, 355–363 (2003).

8) Y. Fukumura, S. Tajima, S. Oshitani, Y. Ushijima, I. Kobayashi, F. Hara, S. Yamamoto, and M. Yabuuchi: Fully enzymatic method for determining 1,5-anhydro-D-glucitol in serum. *Clin. Chem.,* **40**, 2013–2016 (1994).

9) F. Jing, L. Jun, Y. Wang, M. Zhu, Z. Yong, X. Fei, and J. Zhang: A novel fully enzymatic method for determining glucose and 1,5-anhydro-D-glucitol in serum of one cuvette. *Appl. Biochem. Biotechnol.,* **150**, 327–335 (2008).

10) T.H. de Koker, M.D. Mozuch, D. Cullen, J. Gaskell, and P.J. Kersten: Isolation and purification of pyranose 2-oxidase from *Phanerochaete chrysosporium* and characterization of gene structure and regulation. *Appl. Environ. Microbiol.,* **70**, 5794–5800 (2004).

11) O. Spadiut, K. Radakovits, I. Pisanelli, C. Salaheddin, M. Yamabhai, T.C. Tan, C. Divne, and D. Haltrich: A thermostable triple mutant of pyranose 2-oxidase from *Trametes multicolor* with improved properties for biotechnological applications. *Biotechnol. J.,* **4**, 525–534 (2009).

12) N. Hassan, T.C. Tan, O. Spadiut, I. Pisanelli, L. Fusco, D. Haltrich, C.K. Peterbauer, and C. Divne: Crystal structures of *Phanerochaete chrysosporium* pyranose 2-oxidase suggest that the N-terminus acts as a propeptide that assists in homotetramer assembly. *FEBS Open Biol.,* **3**, 496–504 (2013).

13) I. Pisanelli, M. Kujawa, O. Spadiut, R. Kittl, P. Halada, J. Volc, M. D. Mozuch, P. Kersten, D. Haltrich, and C. Peterbauer: Pyranose 2-oxidase from *Phanerochaete chrysosporium*--expression in *E. coli* and biochemical characterization. *J. Biotechnol.,* **142**, 97–106 (2009).

14) O. Spadiut, T.C. Tan, I. Pisanelli, D. Haltrich, and C. Divne: Importance of the gating segment in the substrate-recognition loop of pyranose 2-oxidase. *FEBS J.,* **277**, 2892–2909 (2010).
15) C. Leitner, J. Volc, and D. Haltrich: Purification and characterization of pyranose oxidase from the white rot fungus *Trametes multicolor*. *Appl. Environ. Microbiol.,* **67**, 3636–3644 (2001).
16) S.C. Johnsrud and K.E. Eriksson: Cross-breeding of selected and mutated homokaryotic strains of *Phanerochaete chrysosporium* K-3: New cellulase deficient strains with increased ability to degrade lignin. *Appl. Microbiol. Biotechnol.,* **21**, 320–327 (1985).
17) S.M. Kremer and P.M. Wood: Evidence that cellobiose oxidase from *Phanerochaete chrysosporium* is primarily an Fe(III) reductase. Kinetic comparison with neutrophil NADPH oxidase and yeast flavocytochrome b_2. *Eur. J. Biochem.,* **205**, 133–138 (1992).
18) N. Habu, K. Igarashi, M. Samejima, B. Pettersson, and K.-E.L. Eriksson: Enhanced production of cellobiose dehydrogenase in cultures of *Phanerochaete chrysosporium* supplemented with bovine calf serum. *Biotechnol. Appl. Biochem.,* **26**, 97–102 (1997).
19) K. Igarashi, T. Ishida, C. Hori, and M. Samejima: Characterization of an endoglucanase belonging to a new subfamily of glycoside hydrolase family 45 of the basidiomycete *Phanerochaete chrysosporium*. *Appl. Environ. Microbiol.,* **74**, 5628–5634 (2008).
20) W. Wang and B.A. Malcolm: Two-stage PCR protocol allowing introduction of multiple mutations, deletions and insertions using QuikChange Site-Directed Mutagenesis. *Biotechniques.,* **26**, 680–682 (1999).
21) K. Ozawa, H. Iwasa, N. Sasaki, N. Kinoshita, A. Hiratsuka, and K. Yokoyama: Identification and characterization of thermostable glucose dehydrogenases from thermophilic filamentous fungi. *Appl. Microbiol. Biotechnol.,* **101**, 173–183 (2017).
22) T. Araki, T. Nakatsuka, F. Kobayashi, E. Watanabe-Ishimaru, H. Sanada, T. Tamura, and K. Inagaki: Reactivity of sorbose dehydrogenase from *Sinorhizobium* sp. 97507 for 1,5-anhydro-D-glucitol. *Biosci. Biotechnol. Biochem.,* **79**, 1130–1132 (2015).
23) I. Masuda-Nishimura, T. Minamihara, and Y. Koyama: Improvement in thermal stability and reactivity of pyranose oxidase from *Coriolus versicolor* by random mutagenesis. *Biotechnol. Lett.,* **21**, 203–207 (1999).
24) H. Shibuya, S. Kaneko, and K. Hayashi: A single amino acid substitution enhances the catalytic activity of family 11 xylanase at alkaline pH. *Biosci. Biotechnol. Biochem.,* **69**, 1492–1497 (2005).
25) J.D. Bloom, M.M. Meyer, P. Meinhold, C.R. Otey, D. MacMillan, and F.H. Arnold: Evolving strategies for enzyme engineering. *Curr. Opin. Struct. Biol.,* **15**, 447–452 (2005).
26) M. Tachioka, N. Sugimoto, A. Nakamura, N. Sunagawa, T. Ishida, T. Uchiyama, K. Igarashi, and M. Samejima: Development of simple random mutagenesis protocol for the protein expression system in *Pichia pastoris*. *Biotechnol. Biofuels,* **9**, 199 (2016).
27) N.E. Chayen: Optimization techniques for automation and high throughput. *Methods Mol. Biol.,* **363**, 175–190 (2007).
28) K. Katoh, K. Misawa, K. Kuma, and T. Miyata: MAFFT: a novel method for rapid multiple sequence alignment based on fast Fourier transform. *Nucleic Acids Res.,* **30**, 3059–3066 (2002).
29) K. Katoh and D.M. Standley: MAFFT multiple sequence alignment software version 7: improvements in performance and usability. *Mol. Biol. Evol.,* **30**, 772–780 (2013).
30) O. Trott and A.J. Olson: AutoDock Vina: improving the speed and accuracy of docking with a new scoring function, efficient optimization, and multithreading. *J. Comput. Chem.,* **31**, 455–461 (2010).